Heliyon 10 (2024) e39084

Contents lists available at ScienceDirect

Heliyon

journal homepage: www.cell.com/heliyon

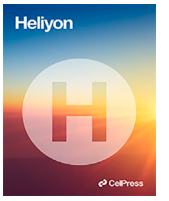

Research article

Bicubic regression analysis a novel approach for estimation of physicochemical properties of skin cancer drugs through degree based entropy

Khalil Hadi Hakami [a], Abdul Rauf Khan [b,*], Iqra Zia [b]

[a] Department of Mathematics, Faculty of Science, Jazan University, P.O. Box 2097, Jazan 45142, Kingdom of Saudi Arabia
[b] Department of Mathematics, Faculty of Sciences, Ghazi University, Dera Ghazi Khan, 32200, Pakistan

ARTICLE INFO

Keywords:
Degree based entropies
Computation
Molecular graph
QSPR analysis
Regression model
Skin cancer drugs
Chemical applications of graph indices

ABSTRACT

Skin cancer poses a significant risk to the healthcare system worldwide and is projected to increase substantially over the next two decades, particularly if not detected in its early stages. The primary aim of this study is to construct a quantitative structure-property relationship (QSPR) by correlating calculated entropies with topological indices and specific physical-chemical properties of pharmaceuticals, in order to enhance their usefulness. The bicubic regression model is constructed through degree-based topological entropies to perform the QSPR analysis for the prediction of physiochemical properties like polar surface area, complexity, molar refractivity, boiling point, and polarity of skin cancer drugs. It is also examined that degree-based entropies provide best-fit models for skin cancer physiochemical properties. We inspected five physiochemical properties of these anticancer drugs and found this methodology suitable for predicting best-fit approximations regarding R^2 value. It is expected that this approach will be very favourable to examining problems related to mathematical chemistry.

1. Introduction

Skin is the body's most important organ. It protects against heat, sunburn, damage, and illness. Moreover, it plays a crucial role in regulating body temperature and acts as a storage site for vitamin D and lipids. The epidermis consists of three different cell types. The epidermis is predominantly composed of thin, flattened cells known as squamous cells. They create melanin, the pigment responsible for the skin's natural colour. Melanocytes increase pigment production in response to sun exposure, resulting in skin darkening or tanning. The dermis contains blood and lymphatic veins, hair follicles, and glands.

Nonmelanoma skin cancers encompass carcinoma of squamous cells and carcinoma of the basal cells. Skin cancer has the potential to occur on any part of the body, however, it is most commonly found on the neck, face, hands, and arms due to prolonged exposure to sunlight. Skin cancer, which is the most common form of cancer in the country, has a significant incidence of illness and death [1].

Inflammatory bowel disease (IBD), a persistent autoimmune illness, is associated with an increased susceptibility to skin cancer. The objective of this study is to assess the level of understanding about skin cancer and the factors that increase the risk of developing it in people with inflammatory bowel disease (IBD) [2]. In addition, we will assess the existing measures taken by the patients to safeguard their skin. This study aims to identify any areas of insufficient awareness among patients with inflammatory bowel illness

* Corresponding author.
E-mail address: khankts@gmail.com (A.R. Khan).

https://doi.org/10.1016/j.heliyon.2024.e39084
Received 24 June 2024; Received in revised form 7 October 2024; Accepted 7 October 2024

Available online 10 October 2024

on the prevention of skin cancer. The incidence of skin cancer appears to be increasing annually. Typically, these skin cancers can be successfully treated.

The prevalence of newly diagnosed melanoma cases has been increasing for at least the past four decades. Melanoma is difficult to treat because it tends to spread to surrounding tissues and other parts of the body. Melanoma and other cancers have different risk factors [3]. The effectiveness of sun avoidance, sunscreen application, and wearing protective clothing in lowering the incidence of skin cancer is currently unknown [4].

Delaying the treatment of NMSCs might lead to considerable morbidity [5]. The pale complexion and blonde hair are both significant risk factors for sunburn and the growth of skin cancer, both externally and internally [6]. The illness also had a substantial influence on a worldwide level. Scientists engage in the arduous task of developing and researching novel medications, which is a complex and demanding endeavour due to its high costs, lengthy duration, and inherent challenges [7]. To address and prevent this life-threatening problem, a multitude of drug investigations are required, and a multitude of drug examinations are conducted to combat these lethal illnesses [8]. Swift identification and immediate administration of medicine are crucial to overcoming the condition [9].

The sickness has a significant impact on the global population as well. Scientists engage in the development and investigation of novel pharmaceuticals, and due to the substantial expenses, lengthy duration, and rigorous nature of this discipline, their research is frequently challenging. Multiple clinical trials are necessary to treat and prevent this lethal condition, and numerous pharmaceutical experiments are carried out to tackle these fatal illnesses. Early identification and prompt delivery of therapy are crucial in combating the sickness. The most effective pharmaceuticals for improving the health of a community are: Binimetinib ($C17H15BrF2N4O3$), encorafenib ($C22H27ClFN7O4S$), dabrafenib ($C23H20F3N5O2S2$), dacarbazine ($C6H10N6O$), fluorouracil ($C4H3FN2O2$), trametinib ($C26H23FIN5O4$), daurismo ($C21H22N6O$), vemurafenib ($C23H18ClF2N3O3S$), imiquimod ($C14H16N4$), odomzo ($C26H32F3N3O11P2$), vismodegib ($C19H14Cl2N2O3S$), picato ($C25H34O6$), and cobimetinib ($C21H21F3IN3O2$) [10].

Cancer is widely recognized as a significant contributor to global mortality, with the occurrence of skin cancer on the rise in nations where these types of malignancies are common. From 1970 to 2007, melanoma saw the second-highest rise in death rate among all known malignancies in Canada. Additionally, it is projected that skin cancer is the most prevalent type of cancer in the USA [11]. By Erb et al. [12], skin cancers are among the most commonly diagnosed malignant tumours in Caucasians globally.

The prevalence of these cancers is continuously rising, primarily due to increasing exposure to ultraviolet (UV) radiation. Skin carcinoma and skin cancers that are not melanoma are among the most common kinds of skin cancer. The prevalence of both types of skin cancer is highest among those with pale skin, blue or green eyes, and blonde or red hair, who are prone to sunburn and have a large number of moles. Exposure to ultraviolet (UV) radiation is the primary environmental risk factor for the development of skin cancer [13].

Basal cell carcinoma (BCC) and squamous cell carcinoma (SCC) are prevalent types of nonmelanoma skin cancer that are widespread worldwide. Globally, there is an estimated annual incidence of approximately two to three million instances of nonmelanoma skin malignancies (NMSCs). Basal cell carcinoma (BCC) is the predominant form of cancer in the United States [6]. Approximately two million new cases of nonmelanoma skin cancer (NMSC) were reported in the United States in 2012, according to estimates. It was discovered that the postponement of therapy resulted in substantial disease and distress. Delaying the treatment of NMSCs might lead to considerable morbidity. Individuals with fair skin tone and blond hair are more susceptible to sunlight and are both extrinsic and intrinsic risk factors for the onset of skin cancer [14].

The theory of graphs is a mathematical discipline that employs graph characteristics to gain a comprehensive understanding of intricate occurrences [15,16]. Chemical graph theory is the utilization of graph theory to examine the structures of molecules [17,18]. Chemical graph theory provides chemists with a vast field of research that allows them to employ graph theory to demonstrate the remarkable properties of chemicals mathematically. Chemical graph theory has diverse applications in medicine, medical research, and scientific investigation [19,20]. Assume a graph $\mathcal{G}_{(V,E)}$ where $\mathcal{V}$ represents the collection of vertices and $\mathcal{E}$ represents the collection of edges. The degree of a vertex, denoted as d_v, is defined by the number of edges that connect to it [21].

Pharmaceuticals are represented as molecular networks in theoretical chemistry, where each vertex is an atom and each edge denotes a relationship between two atoms [22]. QSPR is a highly effective analytical technique to transform a molecule into a series of number values that accurately represent its essential chemical and physical characteristics [23]. Prosanta Sarkar et al. established a quantitative structure-property relationship (QSPR) that correlates degree-based indicators with the physical attributes of hydrocarbons [24]. The study demonstrated that indices can accurately forecast the physical characteristics of hydrocarbons [25].

Quantitative Structure-Property Relationship (QSPR) models are used to estimate the significant level of indices. Researchers created a Quantitative Structure-Property Relationship/Quantitative Structure-Activity Relationship (QSPR/QSAR) model to establish a connection between chemical structure indices and their physical characteristics [26].

Paul et al. compare multiplicative and scalar multiplicative degree-based topological descriptors in terms of entropy measure in [27]. Twelve unique descriptors derived from geometric, harmonic, and Zagreb degree-based descriptors are proposed by Arockiaraj et al. in 2023 [28]. The efficacy of these descriptors is then tested on a data set comprising 55 benzenoid hydrocarbons of environmental concern. In [29], Rahul and Clement give the entropy measure of the carbon allotropes pentagraphene, phagraphene, and phographene. Two-dimensional polymeric phthalocyanine frameworks can be seen in highly ordered organometallic structures known as phthalocyanine derivative nanostructures describe how the growth of these structures is examined to investigate their topological properties using connectivity-based bond additive descriptors [30].

In 1947, Chemist Wiener introduced a topological index by studying how the molecular structure of a certain hydrocarbon molecule relates to its physical and chemical properties [31]. In 2010, the second Zagreb index was recalculated and Damir et al. discovered that it was equivalent to the inverse sum indeg index, as stated in their study [32]. In 2016, Kulli initiated the compu-

tation of valency-based topological indices by employing several Banhatti indices and considering the valency of atom bonds [33–35]. Ranjini initially proposed the concept of redefined Zagreb indices in reference [36], while Shanmukha did so in [37].

2. Material and methods

Our skin is a vital barrier to protect us from harm, disease, moisture, and discomfort. In addition, it helps the body absorb essential nutrients like lipids and sunshine, controls body temperature, and insulates the body and its surroundings. The extra pigment influences the colour of the skin that daylight induces pigment cells to create. Though it can appear anywhere on the skin, skin cancer is most frequently found on the face, neck, and upper extremities due to UV radiation.

Skin cancer is the predominant form of cancer in the country and is linked to a significant mortality and morbidity rate. Blond hair and fair skin are both inherent and extrinsic risk factors for developing skin cancer, as well as having a high tendency to get sunburned. Globally speaking, the illness had a huge effect as well. Scientists study and create new medications, and because this is a costly, time-consuming, and difficult field, its findings are difficult to apply. Several treatment trials are required to tackle these deadly diseases, and several drug tests are conducted to cure and stop this condition. To combat the illness, early detection and fast treatment administration are essential. The top thirteen medications for a community's health are binimetinib, encorafenib, dabrafenib, dacarbazine, fluorouracil, trametinib, daurismo, vemurafenib, imiquimod, odomzo, vismodegib, picato, and cobimetinib. Two classes of cancer growth inhibitors are sorafenib and binimetinib. Their mode of action involves targeting certain proteins that stimulate the proliferation of cancer cells. Through the inhibition of specific proteins, this combination of drugs slows or inhibits the growth of cancer cells.

Imiquimod is a natural chemical name used to describe a new class of drugs known as imidazoquinolones. It has been found to boost human defences and possess potent antitumor and pathogenic qualities. Imiquimod is used to treat actinic keratoses of the face and scalp as well as a specific kind of skin cancer known as superficial basal cell carcinoma. In addition to superficial basal cell carcinoma, imiquimod is effective in treating actinic keratoses, a skin infection that mostly affects the face and scalp. Odomzo (sonidegib) is indicated for the management of adult patients diagnosed with advanced localized basal cell carcinoma (BCC) basal, a kind of skin cancer that has shown improvement after radiation or surgery, or for those who are not suitable candidates for these therapeutic interventions.

One fluoroquinolone used to treat acne is fluorouracil. This medication is used topically to treat malignant and precancerous skin infections. Fluorouracil belongs to a class of drugs called anti-metabolites. It stops the abnormal cells from growing, which is what causes the skin condition. Acute myeloid leukemia (AML), a malignancy of the white blood cells, is treated in adults with daurismo, a cancer medication. When the patient is not responding to conventional chemotherapy, it is combined with a modest dosage of cytarabine, another cancer medication. Metabotropic malignant melanoma is a kind of skin cancer that is treated with dacarbazine, a chemotherapy medication. The medication disrupts malignant cells' natural function by alkylating and halting their DNA. As a cancer growth blocker, vemurafenib belongs to a class of targeted medicinal products. This treatment addresses skin cancer (melanoma) that is incurable or cannot be surgically removed. The molecular structures of skin cancer treatment drugs are shown in Fig. 1 [a-f] and Fig. 2 [a-f], which may be obtained from ChemSpider and PubChem.

A numerical representation of a chemical structure is obtained by computation [38] to determine a topological index. The topological index is a graph invariant that precisely characterizes the topology of a graph [39].

The graph $\mathcal{J}_{(\mathcal{K},\mathcal{F})}$, where the collection of vertices is $\mathcal{K}(\mathcal{J})$ and the collection of edges is $\mathcal{F}(\mathcal{G})$ [40]. The degree of a vertex $\dot{g}_1$ is precisely determined by the number of edges that connect it. This is denoted as $\alpha_{\dot{g}_1}$. The degree of edge $e = \dot{g}_1 \sim \dot{g}_2$ of $\mathcal{J}$ is defined as $\alpha_e = \alpha_{\dot{g}_1} + \alpha_{\dot{g}_2} - 2$ [41]. In graph theory, a molecular graph also referred to as a chemical network, is a simple network where vertices and edges correspond to individual atoms and chemical bonds [42]. Through the analysis of the vertices and edges of the molecular structure $\mathcal{J}$, we divide the edge group $K(J)$ into segments of the subsequent kinds $\mathcal{K}^{(\dot{g}_1,\dot{g}_2)} = \left\{ \dot{e} = \dot{g}_1 \sim \dot{g}_2 \in \mathcal{K}(\mathcal{J}) \mid \dot{g}_1 = \alpha_{\dot{g}_1},\ \dot{g}_2 = \alpha_{\dot{g}_2} \right\}$.

Shannon introduced the notion of entropy in 1948 [43], which quantifies the level of molecular disorder within a system [44]. Entropy measures the amount of thermal energy per unit temperature in a system that cannot be used for useful work [45,46]. Entropy is used to quantify the molecular disorder of the system [47,48].

The measurement of edge-weighted graph entropy was initially presented in 2009 [49] for an edge-weighted graph $\mathcal{J} = ((\mathcal{V}, \mathcal{E}), \psi(Q_{\dot{g}_1} Q_{\dot{g}_2}))$, where $\psi(Q_{\dot{g}_1} Q_{\dot{s}_2})$ denotes the edge-weight of an edge $(Q_{\dot{g}_1} Q_{\dot{g}_2})$. The entropy of a $\mathcal{J}$ is defined by the formula

$$ENT_{\psi}(\mathcal{J}) = -\sum_{\dot{g}_1 \sim \dot{g}_2} \frac{\psi(Q_{\dot{g}_1\dot{g}_2})}{\sum_{\dot{g}_1 \sim \dot{g}_2} \psi(Q_{\dot{g}_1\dot{g}_2})} log\left[\frac{\psi(Q_{\dot{g}_1\dot{g}_2})}{\sum_{\dot{g}_1 \sim \dot{g}_2} \psi(Q_{\dot{g}_1\dot{g}_2})}\right]$$

$$= log\left[\sum_{\dot{g}_1 \sim \dot{g}_2} \psi(Q_{\dot{g}_1\dot{g}_2})\right] - \frac{1}{\sum_{\dot{g}_1 \sim \dot{g}_2} \psi(Q_{\dot{g}_1\dot{g}_2})} log\left[\prod_{\dot{g}_1 \sim \dot{g}_2} |\mathcal{E}_{i,j}| \psi(Q_{\dot{g}_1\dot{g}_2})^{\psi(Q_{\dot{g}_1\dot{g}_2})}\right]$$

1^{st} redefined Zagreb polynomial, index and entropy

$$ReZG_1(\mathcal{J}, \kappa) = \sum_{\dot{g}_1 \sim \dot{g}_2} \kappa^{\frac{\chi_{\dot{g}_1} + \chi_{\dot{g}_2}}{\chi_{\dot{g}_1} \times \chi_{\dot{g}_2}}} \tag{1}$$

$$ReZG_1(\mathcal{J}) = \sum_{\dot{g}_1 \sim \dot{g}_2} \frac{\chi_{\dot{g}_1} + \chi_{\dot{g}_2}}{\chi_{\dot{g}_1} \times \chi_{\dot{g}_2}} \tag{2}$$

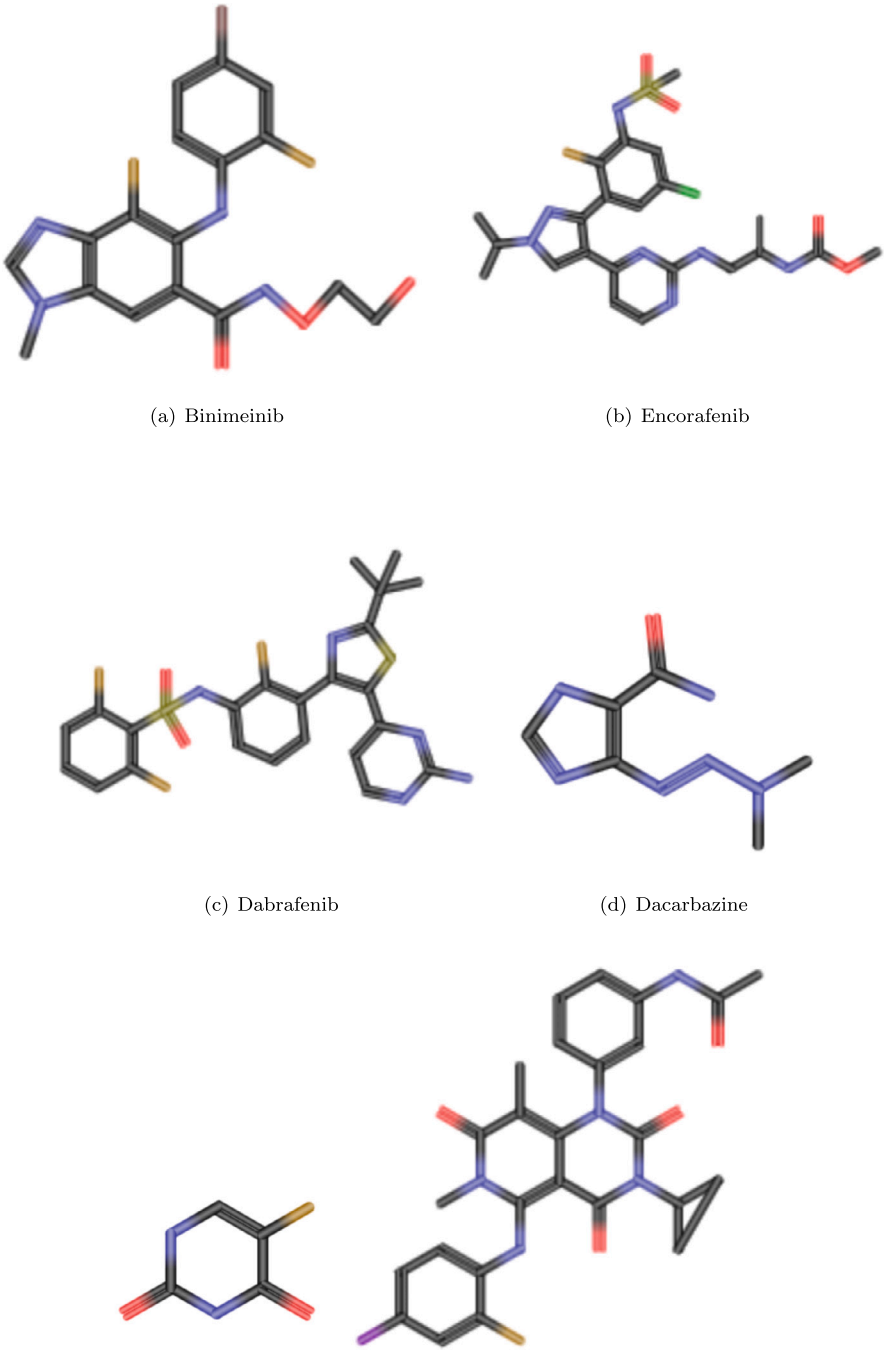

(a) Binimeinib (b) Encorafenib

(c) Dabrafenib (d) Dacarbazine

(e) Fluorouracil (f) Trametinib

Fig. 1. Molecular Structures of Skin Cancer Treatment Drugs.

$$ENT_{ReZG_1}(\mathcal{J}) = \log(ReZG_1) - \frac{1}{ReZG_1}\log\left\{\prod_{\dot{g}_1\sim\dot{g}_2}|\mathcal{E}_{i,j}|[\frac{\chi_{\dot{g}_1}+\chi_{\dot{g}_2}}{\chi_{\dot{g}_1}\chi_{\dot{g}_2}}]^{[\frac{\chi_{\dot{g}_1}+\chi_{\dot{g}_2}}{\chi_{\dot{g}_1}\chi_{\dot{g}_2}}]}\right\} \tag{3}$$

2^{nd} redefined Zagreb polynomial, index and entropy

$$ReZG_2(\mathcal{J},\kappa) = \sum_{\dot{g}_1\sim\dot{g}_2}\kappa^{\frac{\chi_{\dot{g}_1}\times\chi_{\dot{g}_2}}{\chi_{\dot{g}_1}+\chi_{\dot{g}_2}}} \tag{4}$$

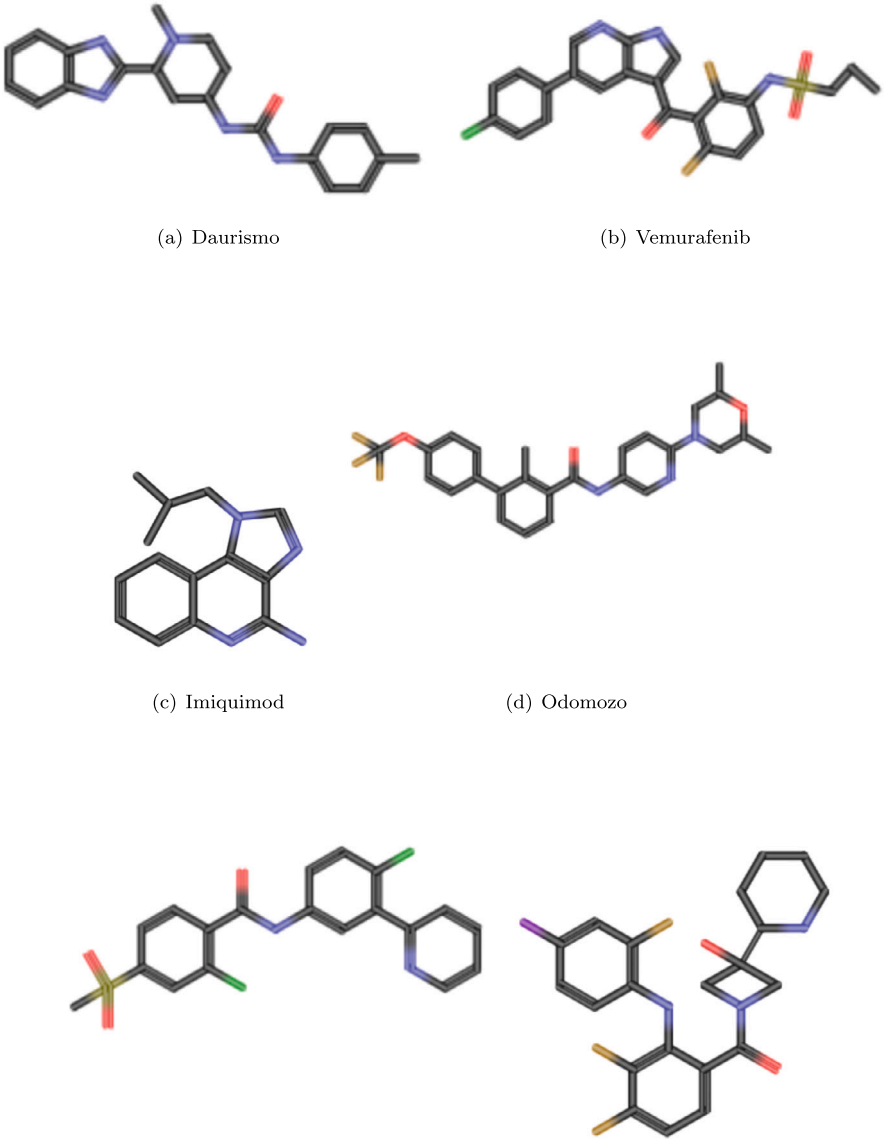

(a) Daurismo (b) Vemurafenib

(c) Imiquimod (d) Odomozo

(e) Vismodegib (f) Cobimetinib

Fig. 2. Molecular Structures of Skin Cancer Treatment Drugs.

$$ReZG_2(\mathcal{J}) = \sum_{\dot{g}_1 \sim \dot{g}_2} \frac{\chi_{\dot{g}_1} \times \chi_{\dot{g}_2}}{\chi_{\dot{g}_1} + \chi_{\dot{g}_2}} \tag{5}$$

$$ENT_{ReZG_2}(\mathcal{J}) = \log(ReZG_2) - \frac{1}{ReZG_2} \log\left\{ \prod_{\dot{g}_1 \sim \dot{g}_2} |\mathcal{E}_{i,j}| [\frac{\chi_{\dot{g}_1} \chi_{\dot{g}_2}}{\chi_{\dot{g}_1} + \chi_{\dot{g}_2}}]^{[\frac{\chi_{\dot{g}_1} \chi_{\dot{g}_2}}{\chi_{\dot{g}_1} + \chi_{\dot{g}_2}}]} \right\} \tag{6}$$

Atom-bond sum connectivity polynomial, index and entropy

$$ABS(\mathcal{J}, \kappa) = \sum_{\dot{g}_1 \sim \dot{g}_2} \kappa^{\sqrt{\frac{(\chi_{\dot{g}_1} + \chi_{\dot{g}_2} - 2)}{(\chi_{\dot{g}_1} + \chi_{\dot{g}_2})}}} \tag{7}$$

$$ABS(\mathcal{J}) = \sum_{\dot{g}_1 \sim \dot{g}_2} \sqrt{\frac{(\chi_{\dot{g}_1} + \chi_{\dot{g}_2} - 2)}{(\chi_{\dot{g}_1} + \chi_{\dot{g}_2})}} \tag{8}$$

Table 1
Atom bond partition of Imiquimod.

Edge partition ($\mathcal{E}_{i,j}$)	Cardinality ($\lvert\mathcal{E}_{i,j}\rvert$)	Edge degree
(1 , 3)	3	2
(2 , 2)	4	2
(2 , 3)	8	3
(3 , 3)	5	4

$$ENT_{ABS(\mathcal{J})}(\mathcal{J}) = \log(ABS(\mathcal{J})) - \frac{1}{ABS(\mathcal{J})}\log\left\{\prod_{\dot{g}_1,\dot{g}_2}|\mathcal{E}_{i,j}|\left(\sqrt{\frac{\chi_{\dot{g}_1}+\chi_{\dot{g}_2}-2}{\chi_{\dot{g}_1}+\chi_{\dot{g}_2}}}\right)^{\left(\sqrt{\frac{\chi_{\dot{g}_1}+\chi_{\dot{g}_2}-2}{\chi_{\dot{g}_1}+\chi_{\dot{g}_2}}}\right)}\right\} \tag{9}$$

1^{st} K-Banhatti polynomial, index and entropy

$$B_1(\mathcal{J},\kappa) = \sum_{\dot{g}_1\sim\dot{g}_2}\kappa^{(\chi_{\dot{g}_1}+\chi_{\dot{e}})} \tag{10}$$

$$B_1(\mathcal{J}) = \sum_{\dot{g}_1\sim\dot{g}_2}(\chi_{\dot{g}_1}+\chi_{\dot{e}}) \tag{11}$$

$$ENT_{B_1(\mathcal{J})}(\mathcal{J}) = \log(B_1(\mathcal{J})) - \frac{1}{B_1(\mathcal{J})}\log\left\{\prod_{\dot{g}_1\sim\dot{g}_2}|\mathcal{E}_{i,j}|[\chi_{\dot{g}_1}+\chi_{\dot{e}}]^{[\chi_{\dot{g}_1}+\chi_{\dot{e}}]}\right\} \tag{12}$$

2^{nd} K-Banhatti polynomial, index and entropy

$$B_2(\mathcal{J},\kappa) = \sum_{\dot{h}_1\sim\dot{h}_2}\kappa^{(\chi_1\times\chi_{\dot{e}})} \tag{13}$$

$$B_2(\mathcal{J}) = \sum_{\dot{h}_1\sim\dot{h}_2}(\chi_1\times\chi_{\dot{e}}) \tag{14}$$

$$ENT_{B_2(\mathcal{J})} = \log(B_2(\mathcal{J})) - \frac{1}{B_2(\mathcal{J})}\log\left\{\prod_{\dot{g}_1\sim\dot{g}_2}|\mathcal{E}_{i,j}|[\chi_{\dot{g}_1}\times\chi_{\dot{e}}]^{[\chi_{\dot{g}_1}\times\chi_{\dot{e}}]}\right\} \tag{15}$$

3. Results

This section presents the results of our investigation.

3.1. Computation of degree-based entropies

In this section, we calculated the entropies of Imiquimod based on its degree.

The 1^{st} redefined Zagreb entropy measure of $(\mathcal{IQ})$

Utilizing of Equation (1) and Table 1, we obtain:

$$ReZG_1(\mathcal{IQ},\kappa) = (3)\kappa^{\frac{4}{3}} + (4)\kappa^{\frac{4}{4}} + (8)\kappa^{\frac{5}{6}} + (5)\kappa^{\frac{6}{9}} \tag{16}$$

Taking the derivative of Equation (16) at $\kappa = 1$ along with Equation (2), we have

$$ReZG_1(\mathcal{IQ}) = 18$$

Utilizing of Equation (3) and Table 1, we obtain:

$$ENT_{ReZG_1}(\mathcal{IQ}) = \log(18) - \frac{1}{(18)}\log\left\{(3)(\frac{4}{3})^{\frac{4}{3}}\times(4)(\frac{4}{4})^{\frac{4}{4}}\times(8)(\frac{5}{6})^{\frac{5}{6}}\times(5)(\frac{6}{9})^{\frac{6}{9}}\right\}.$$

$$ReZG_1(\mathcal{IQ}) = 1.1072$$

The 2^{nd} redefined Zagreb entropy measure of $(\mathcal{IQ})$

When use Equation (4) and Table 1, we have

$$ReZG_2(\mathcal{IQ},\kappa) = (3)\kappa^{\frac{3}{4}} + (4)\kappa^{\frac{4}{4}} + (8)\kappa^{\frac{6}{5}} + (5)\kappa^{\frac{9}{6}} \tag{17}$$

differentiating Equation (17) at $\kappa = 1$ along with Equation (5), we obtain

$$ReZG_2(\mathcal{IQ}) = \frac{467}{20}$$

Using Equation (6) and Table 1, we have

$$ENT_{ReZG_2}(\mathcal{IQ}) = \log(\frac{467}{20}) - \frac{1}{\frac{467}{20}} \log\left\{(3)(\frac{3}{4})^{\frac{3}{4}} \times (4)(\frac{4}{4})^{\frac{4}{4}} \times (8)(\frac{6}{5})^{\frac{6}{5}} \times (5)(\frac{9}{6})^{\frac{9}{6}}\right\}$$

$$ReZG_2(\mathcal{IQ}) = 1.242$$

Atom-bond sum connectivity entropy measure of $(\mathcal{IQ})$

Equation (7) and Table 1 are used to obtain:

$$ABS(\mathcal{IQ}, \kappa) = (3)\kappa^{\sqrt{\frac{1}{2}}} + (4)\kappa^{\sqrt{\frac{1}{2}}} + (8)\kappa^{\sqrt{\frac{3}{5}}} + (5)\kappa^{\sqrt{\frac{2}{3}}} \tag{18}$$

When differentiate Equation (18) at $\kappa = 1$ along with Equation (8), then get:

$$ABS(\mathcal{IQ}) = (3)\sqrt{\frac{1}{2}} + (4)\sqrt{\frac{1}{2}} + (8)\sqrt{\frac{3}{5}} + (5)\sqrt{\frac{2}{3}}$$

$$ABS(\mathcal{IQ}) = 15.22$$

Utilizing Equation (9) and Table 1

$$ENT_{ABS}(\mathcal{IQ}) = \log(ABS) - \frac{1}{ABS} \log\left\{(3)(\sqrt{\frac{1}{2}})^{\sqrt{\frac{1}{2}}} \times (4)(\sqrt{\frac{1}{2}})^{\sqrt{\frac{1}{2}}} \times (8)(\sqrt{\frac{3}{5}})^{\sqrt{\frac{3}{5}}} \times (5)(\sqrt{\frac{2}{3}})^{\sqrt{\frac{2}{3}}}\right\}.$$

$$ABS(\mathcal{IQ}) = 1.0306$$

The 1^{st} K**-Banhatti entropy measure of** $(\mathcal{IQ})$

Equation (10) and Table 1 give:

$$B_1(\mathcal{IQ}, \kappa) = (3)\kappa^8 + (4)\kappa^8 + (8)\kappa^{11} + (5)\kappa^{14} \tag{19}$$

When differentiate Equation (19) at $\kappa = 1$ along with Equation (11), we have:

$$B_1(\mathcal{IQ}) = 214$$

Utilizing Equation (12) and Table 1, we obtain

$$ENT_{B_1}(\mathcal{IQ}) = \log(214) - \frac{1}{(214)} \log\left\{(3)(8)^8 \times (4)(8)^8 \times (8)(11)^{11} \times (5)(14)^{14}\right\}$$
$$= 2.1218$$

The 2^{nd} K**-Banhatti entropy measure of** $(\mathcal{IQ})$

Equation (13) and Table 1 are used to get:

$$B_2(\mathcal{IQ}, \kappa) = (3)\kappa^{[(1\times2)+(3\times2)]} + (4)\kappa^{[(2\times2)+(2\times2)]} + (8)\kappa^{[(2\times3)+(3\times3)]} + (5)\kappa^{[(3\times4)+(3\times4)]} \tag{20}$$

When differentiate Equation (20) at $\kappa = 1$ along with Equation (14), we get:

$$B_2(\mathcal{IQ}) = 296$$

Equation (15) and Table 1 are used to get:

$$ENT_{B_2}(\mathcal{IQ}) = \log(296) - \frac{1}{296} \log\left\{(3)(8^8) \times (4)8^8 \times (8)15^{15} \times (5)24^{24}\right\}.$$
$$= 2.2419$$

Similarly, entropies may be computed for other drugs and their computation values are reflected in Table 3.

4. QSPR analysis

The main objective of this section is to determine a quantitative correlation between the physical-chemical characteristics of the antibiotics recorded in Table 2 and the calculated entropies. These modifications are implemented to improve the efficiency of the topological indices shown in Table 3.

Table 3 presents the computational values of entropies for skin cancer medications, and Fig. 3 analyzes the graphical depiction of the entropies values.

Table 2
Physicochemical properties of skin cancer drugs.

Drugs/Properties	BP (C^o)	MR (cm^3)	P (cm^3)	Complexity	PSA (A^2)
Encorafenib	456.7	71	28.2	294	57
Trametinib	456.3	46.2	18.3	215	100
Dabrafenib		134.1	53.2	836	149
Imiquimod				691	
Vismodegib	561.6	105.5	41.8	625	85
Fluorouracil	653.7	127.4	50.5	817	147
Binimetinib	711.4	121.6	48.2	790	100
Vemurafenib	633.4	106.9	42.4	595	97
Dacarbazine	565.9	115.3	45.7	624	65
odomzo		141.5	56.1	10.9	102
Cobimetinib		96.6	38.3	521	88
Daurismo		25.9	10.2	199	58

Table 3
Computational values of degree-based entropies.

Drugs/Entopies	$Ent(ReZG_1)$	$Ent(ReZG_2)$	$Ent(ABS)$	$Ent(B_1)$	$Ent(B_2)$
Binimetinib	1.2844	1.3978	1.2992	2.3007	2.4289
Encorafenib	1.4441	1.5342	1.3572	2.4196	2.5295
Cobimetinib	1.3601	1.4689	1.2812	2.2952	2.3671
Dabrafenib	1.4289	1.5196	1.3343	2.4039	2.5018
Dacarbazine	1.3585	0.977	0.8193	1.7639	1.8051
Fluorouracil	0.8361	0.8392	0.7235	1.4761	1.4929
Trametinib	1.4646	1.6015	1.3874	2.5562	2.7067
Daurismo	1.3267	1.4412	1.2419	2.3501	2.4523
Vemurafenib	1.4006	1.5164	1.3167	2.3938	2.5360
Imiquimod	1.1072	1.242	1.0306	2.1218	2.2419
Odomzo	1.439	1.541	1.3622	2.4280	2.5457
Vismodegib	1.2683	1.3932	1.2131	2.2406	2.3036

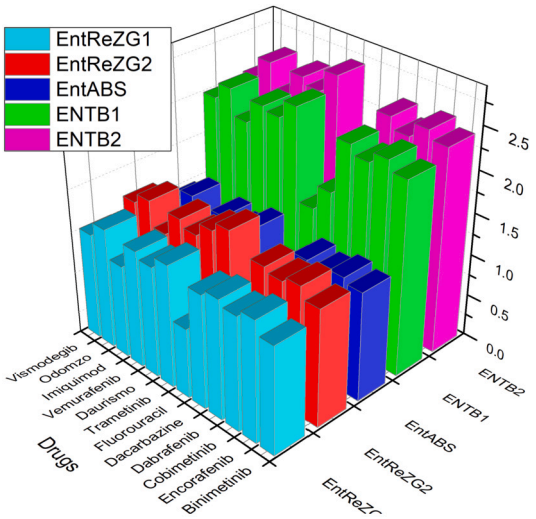

Fig. 3. Graphical Analysis of Outcomes of Entropies.

4.1. Bicubic regression analysis

In some models, regression is used to fit curves instead of straight lines. This method is called curvilinear regression analysis. The bicubic regression method shown in Equation (21) is employed in this study to analyze the physical properties.

$$S = \tau + \tau_1(\mathcal{ENT}_{\mathcal{TI}}) + \tau_2(\mathcal{ENT}_{\mathcal{TI}})^2 + \tau_3(\mathcal{ENT}_{\mathcal{TI}})^3 + \tau_4(\mathcal{ENT}_{\mathcal{TI}})^4 + \tau_5(\mathcal{ENT}_{\mathcal{TI}})^5 + \tau_6(\mathcal{ENT}_{\mathcal{TI}})^6 \tag{21}$$

Table 4
BCR Equations & R^2 value for Boiling Point.

Bicubic Regression Equations	Entropy	R^2
$y = 2E+08x^6 - 2E+09x^5 + 5E+09x^4 - 8E+09x^3 + 8E+09x^2 - 4E+09x + 8E+08$	$Ent(ReZG_1)$	0.9967
$y = -2E+07x^6 + 2E+08x^5 - 6E+08x^4 + 1E+09x^3 - 1E+09x^2 + 5E+08x - 1E+08$	$Ent(ReZG_2)$	0.9979
$y = -2E+06x^6 + 1E+07x^5 - 5E+07x^4 + 7E+07x^3 - 7E+07x^2 + 3E+07x - 6E+06$	$Ent(ABS)$	0.9992
$y = 2E+06x^6 - 2E+07x^5 + 8E+07x^4 - 2E+08x^3 + 2E+08x^2 - 2E+08x + 5E+07$	$Ent(B_1)$	1
$y = -5E+07x^6 + 6E+08x^5 - 3E+09x^4 + 8E+09x^3 - 1E+10x^2 + 1E+10x - 1E+09$	$Ent(B_2)$	0.9981

Table 5
BCR Equations & R^2 value for Polar Surface Area.

Bicubic Regression Equations	Entropy	R^2
$y = 6E+07x^6 - 5E+08x^5 + 1E+09x^4 - 3E+09x^3 + 2E+09x^2 - 1E+09x + 2E+08$	$Ent(ReZG_1)$	0.9984
$y = -6E+07x^6 + 5E+08x^5 - 2E+09x^4 + 3E+09x^3 - 4E+09x^2 + 2E+09x - 5E+08$	$Ent(ReZG_2)$	0.9993
$y = 1E+07x^6 - 7E+07x^5 + 2E+08x^4 - 3E+08x^3 + 2E+08x^2 - 1E+08x + 2E+07$	$Ent(ABS)$	0.9994
$y = 762423x^6 - 1E+07x^5 + 5E+07x^4 - 1E+08x^3 + 2E+08x^2 - 2E+08x + 6E+07$	$Ent(B_1)$	1
$y = -1E+07x^6 + 1E+08x^5 - 7E+08x^4 + 2E+09x^3 - 3E+09x^2 + 2E+09x - 8E+08$	$Ent(B_2)$	0.9688

Table 6
BCR Equations & R^2 value for Complexity.

Bicubic Regression Equations	Entropy	R^2
$y = 2E+08x^6 - 1E+09x^5 + 5E+09x^4 - 8E+09x^3 + 7E+09x^2 - 4E+09x + 7E+08$	$Ent(ReZG_1)$	0.9997
$y = -3E+07x^6 + 2E+08x^5 - 8E+08x^4 + 1E+09x^3 - 1E+09x^2 + 6E+08x - 1E+08$	$Ent(ReZG_2)$	1
$y = -4E+07x^6 + 2E+08x^5 - 7E+08x^4 + 1E+09x^3 - 8E+08x^2 + 4E+08x - 7E+07$	$Ent(ABS)$	0.9998
$y = 4E+06x^6 - 5E+07x^5 + 3E+08x^4 - 7E+08x^3 + 1E+09x^2 - 9E+08x + 3E+08$	$Ent(B_1)$	1
$y = -8E+07x^6 + 1E+09x^5 - 5E+09x^4 + 1E+10x^3 - 2E+10x^2 + 2E+10x - 5E+09$	$Ent(B_2)$	0.9992

In the above methods, $\mathcal{S}$ is the physio-chemical property, regression constants are represented by τ and τ_k where $k = 1,2,3,4,5,6$ and $\mathcal{ENT}_{\mathcal{TI}}$ shows topological index value. Table 4 comprises **BCR** Equations & R^2 value for Boiling Point of skin cancer treatment drugs.

Table 5 comprises **BCR** Equations & R^2 value for PSA of skin cancer treatment drugs. Table 6 comprises **BCR** Equations & R^2 value for Complexity of skin cancer treatment drugs. Table 7 comprises **BCR** Equations & R^2 value for Molar Refraction of skin cancer treatment drugs. Table 8 comprises **BCR** Equations & R^2 value for Polarity of skin cancer treatment drugs. In Fig. 4 **BCR** Models of Boiling Point are presented. In Fig. 5 **BCR** Models of Polar Surface Area are presented. In Fig. 6 **BCR** Models of Complexity are presented. In Fig. 7 **BCR** Models of Molar Refraction are presented. In Fig. 8 **BCR** Models of Polarity are presented.

5. Discussions

The primary aim of this study is to conduct a QSPR analysis to estimate the physicochemical characteristics of medications used to treat skin cancer. This study examines the physicochemical features of twelve skin cancer treatment drugs, including boiling point, molar refraction, polarity, complexity, and polar surface area. A novel technique called bicubic regression analysis is employed to estimate physical and chemical characteristics. Furthermore, bicubic regression analysis is conducted using degree-based entropies.

Table 7
BCR Equations & R^2 value for Molar Refraction.

Bicubic Regression Equations	Entropy	R^2
$y = 1E+07x^6 - 8E+07x^5 + 3E+08x^4 - 4E+08x^3 + 4E+08x^2 - 2E+08x + 4E+07$	$Ent(ReZG_1)$	0.9995
$y = -991938x^6 + 8E+06x^5 - 3E+07x^4 + 5E+07x^3 - 5E+07x^2 + 3E+07x - 5E+06$	$Ent(ReZG_2)$	0.9995
$y = -2E+06x^6 + 1E+07x^5 - 3E+07x^4 + 5E+07x^3 - 4E+07x^2 + 2E+07x - 3E+06$	$Ent(ABS)$	0.9996
$y = 614145x^6 - 7E+06x^5 + 3E+07x^4 - 7E+07x^3 + 1E+08x^2 - 7E+07x + 2E+07$	$Ent(B_1)$	1
$y = -1E+07x^6 + 1E+08x^5 - 6E+08x^4 + 2E+09x^3 - 2E+09x^2 + 2E+09x - 6E+08$	$Ent(B_2)$	0.9978

Table 8
BCR Equations & R^2 value for Polarity.

Bicubic Regression Equations	Entropy	R^2
$y = 4E+06x^6 - 3E+07x^5 + 1E+08x^4 - 2E+08x^3 + 2E+08x^2 - 8E+07x + 2E+07$	$Ent(ReZG_1)$	0.9985
$y = -401116x^6 + 3E+06x^5 - 1E+07x^4 + 2E+07x^3 - 2E+07x^2 + 1E+07x - 2E+06$	$Ent(ReZG_2)$	0.9997
$y = -608928x^6 + 4E+06x^5 - 1E+07x^4 + 2E+07x^3 - 2E+07x^2 + 7E+06x - 1E+06$	$Ent(ABS)$	1
$y = 242251x^6 - 3E+06x^5 + 1E+07x^4 - 3E+07x^3 + 4E+07x^2 - 3E+07x + 8E+06$	$Ent(B_1)$	1
$y = -4E+06x^6 + 5E+07x^5 - 2E+08x^4 + 6E+08x^3 - 1E+09x^2 + 8E+08x - 2E+08$	$Ent(B_2)$	0.9913

Table 9
The Correlation among Entropies and Physicochemical Characteristics of Skin Cancer Treatment Drugs.

Molecular Descriptor	Correlation value	Property
$Ent(RezG_1)$	0.9983	
$Ent(RezG_2)$	0.9989	
$Ent(ABS)$	0.9996	BP
$Ent(B_1)$	1.0000	
$Ent(B_2)$	0.9990	
$Ent(RezG_1)$	0.9997	
$Ent(RezG_2)$	0.9997	
$Ent(ABS)$	0.9998	MR
$Ent(B_1)$	0.9999	
$Ent(B_2)$	0.9989	
$Ent(RezG_1)$	0.9992	
$Ent(RezG_2)$	0.9998	
$Ent(ABS)$	1.0000	P
$Ent(B_1)$	1.0000	
$Ent(B_2)$	0.9956	
$Ent(RezG_1)$	0.9998	
$Ent(RezG_2)$	1.0000	
$Ent(ABS)$	0.9999	Complexity
$Ent(B_1)$	1.0000	
$Ent(B_2)$	0.9996	
$Ent(RezG_1)$	0.9992	
$Ent(RezG_2)$	0.9996	
$Ent(ABS)$	0.9997	PSA
$Ent(B_1)$	1.0000	
$Ent(B_2)$	0.9843	

This technique offers the most accurate estimation for the specified physicochemical parameters. The correlation between degree-based entropies and physicochemical parameters is presented in Table 9.

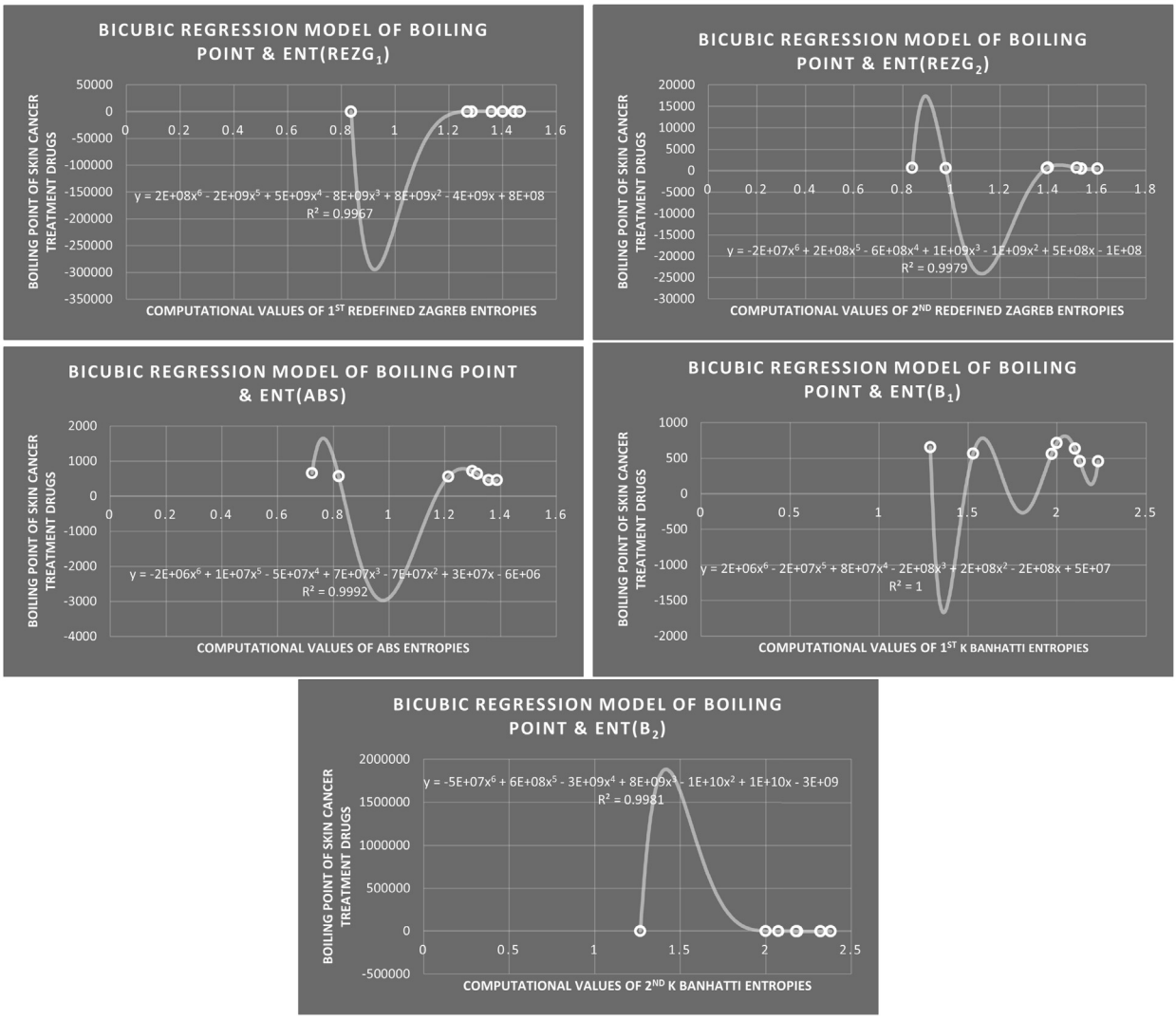

Fig. 4. BCR Models of Boiling Point.

6. Conclusion

This study presents multiple entropy metrics associated with the types of drugs utilized for treating skin cancer. The data gathered were used for quantitative structure-property relationship (QSPR) analysis, which resulted in the development of bicubic regression ($\mathbb{BCR}$) models. These models provide the most precise estimation of the physicochemical characteristics of Pharmaceuticals employed in the treatment of skin cancer. The biquadratic regression approach, in conjunction with degree-based entropies, provided the most accurate estimations for the physicochemical characteristics of drugs employed in the treatment of skin cancer. Based on correlation in Table 9, we may further explain the study's conclusions as follows:

- $Ent(ReZG_1)$ provides best approximations for BP, MR, P, Complexity and PSA
- $Ent(ReZG_2)$ provides best approximations for BP, MR, P, Complexity and PSA
- $Ent(ABS)$ provides best approximations for BP, MR, P, Complexity and PSA
- $Ent(B_1)$ provides best approximations for BP, MR, P, Complexity and PSA
- $Ent(B_1)$ provides best approximations for BP, MR, P, Complexity and PSA

This work uncovers novel opportunities for further research.

CRediT authorship contribution statement

Khalil Hadi Hakami: Writing – review & editing, Visualization, Validation, Software, Resources, Methodology, Investigation, Formal analysis, Data curation, Conceptualization. **Abdul Rauf Khan:** Writing – review & editing, Visualization, Validation, Supervi-

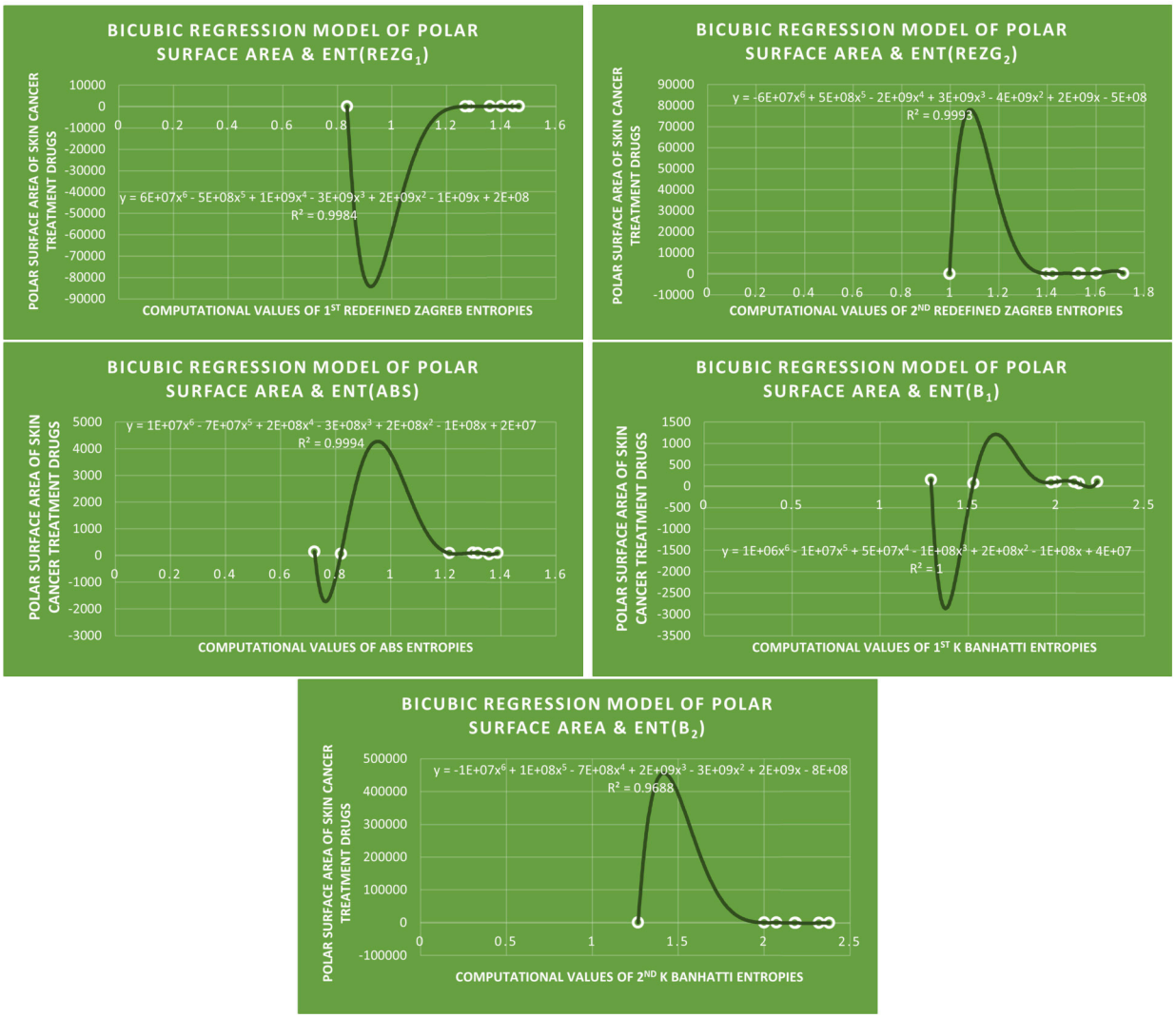

Fig. 5. BCR Models of Polar Surface Area.

sion, Software, Resources, Methodology, Investigation, Formal analysis, Data curation, Conceptualization. **Iqra Zia:** Writing – original draft, Visualization, Validation, Software, Resources, Methodology, Investigation, Formal analysis, Data curation, Conceptualization.

Ethical approval

Not applicable.

Declaration of generative AI and AI-assisted technologies in the writing process

The authors declare they have not used Artificial Intelligence (AI) tools in the creation of this article.

Funding

The authors gratefully acknowledge the funding of the Deanship of Graduate Studies and Scientific Research, Jazan University, Saudi Arabia, through Project Number: GSSRD-24.

Declaration of competing interest

The authors declare that they have no known competing financial interests or personal relationships that could have appeared to influence the work reported in this paper.

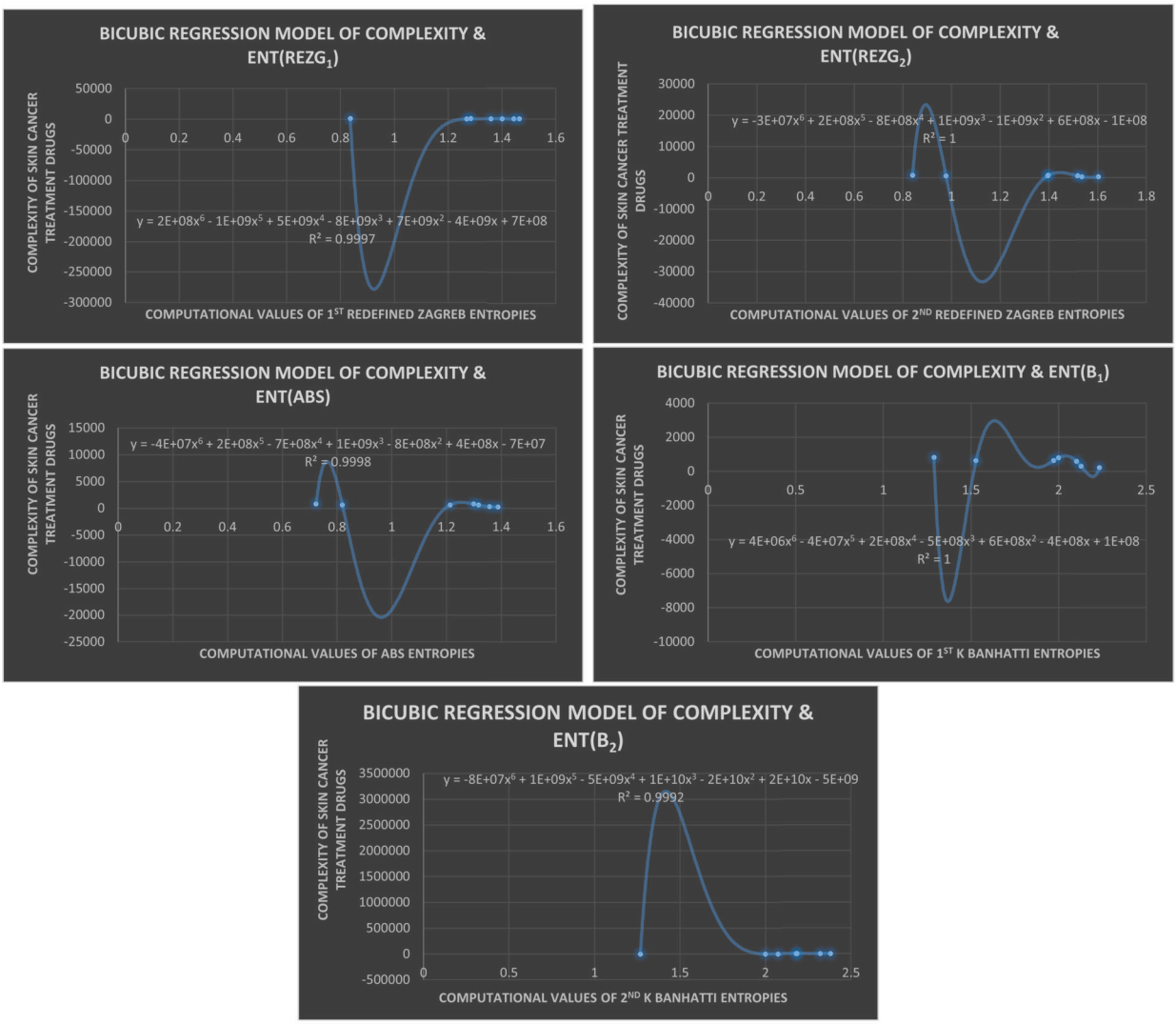

Fig. 6. BCR Models of Complexity.

Data availability

No data was used for the research described in the article.

References

[1] M.F. Simoes, J.S. Sousa, A.C. Pais, Skin cancer and new treatment perspectives: a review, Cancer Lett. 357 (1) (2015) 8–42;
J.N. Kimmel, T.H. Taft, L. Keefer, Inflammatory bowel disease and skin cancer: an assessment of patient risk factors, knowledge, and skin practices, J. Skin Cancer 2016 (2016).

[2] J. Kimmel, T. Taft, L. Keefer, Inflammatory bowel disease and skin cancer: an assessment of patient risk factors, knowledge, and skin practices: 1916, Off. J. Am. Coll. Gastroenterol. ACG 110 (2015) S814–S815.

[3] S. Gandini, F. Sera, M.S. Cattaruzza, P. Pasquini, R. Zanetti, C. Masini, et al., Meta-analysis of risk factors for cutaneous melanoma: III. Family history, actinic damage and phenotypic factors, Eur. J. Cancer 41 (14) (2005) 2040–2059.

[4] D.R. Green, Apoptosis: Physiology and Pathology, Cambridge University Press, 2011.

[5] L.E. Dubas, A. Ingraffea, Nonmelanoma skin cancer, Facial Plast. Surg. Clin. 21 (1) (2013) 43–53.

[6] R.V. Patel, A. Frankel, G. Goldenberg, An update on nonmelanoma skin cancer, J. Clin. Aesthet. Dermatol. 4 (2) (2011) 20.

[7] C.X. Chen, J. Zhu, Z. Zeng, Use of ultrasound to observe mycosis fungoides: a case report and review of literature, Curr. Med. Imag. 18 (7) (2022) 771–775, https://doi.org/10.2174/1573405617666211208121419.

[8] S. Chen, I. Semenov, F. Zhang, Y. Yang, J. Geng, X. Feng, et al., An effective framework for predicting drug–drug interactions based on molecular substructures and knowledge graph neural network, Comput. Biol. Med. 169 (2024) 107900.

[9] Z. Jiang, X. Han, C. Zhao, S. Wang, X. Tang, Recent advance in biological responsive nanomaterials for biosensing and molecular imaging application, Int. J. Mol. Sci. 23 (3) (2022) 1923, https://doi.org/10.3390/ijms23031923.

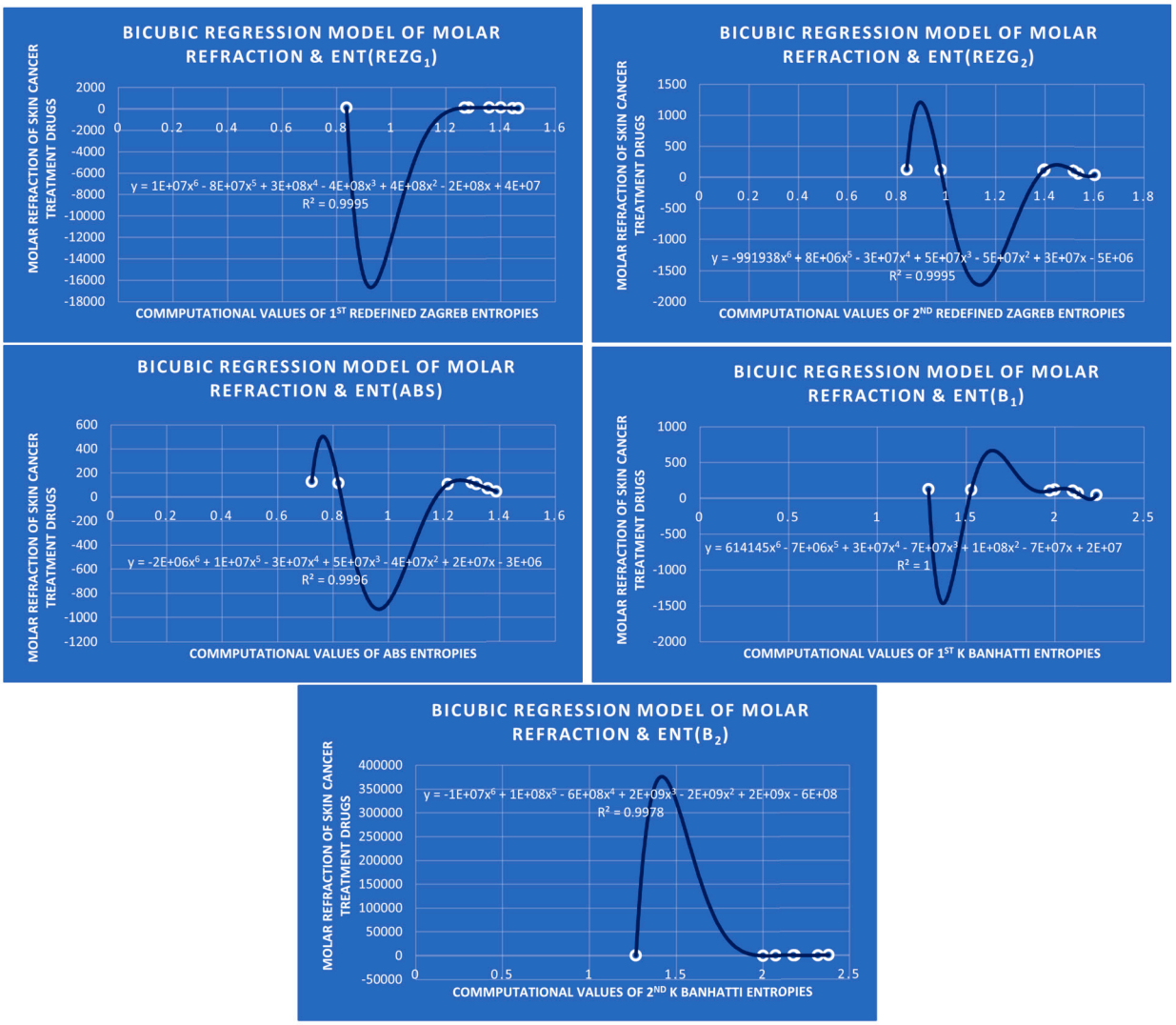

Fig. 7. BCR Models of Molar Refraction.

[10] A.R. Khan, N.U.H. Awan, M.U. Ghani, S.M. Eldin, H. Karamti, A.H. Jawhari, Y.E. Mukhrish, Fundamental aspects of skin cancer drugs via degree-based chemical bonding topological descriptors, Molecules 28 (9) (2023) 3684.

[11] L. Kachuri, P. De, L.F. Ellison, R. Semenciw, Cancer incidence, mortality and survival trends in Canada, 1970-2007, Chronic Dis. Inj. Can. 33 (2) (2013).

[12] P. Erb, J. Ji, M. Wernli, E. Kump, A. Glaser, S.A. Büchner, Role of apoptosis in basal cell and squamous cell carcinoma formation, Immunol. Lett. 100 (1) (2005) 68–72.

[13] S. Gandini, D. Palli, G. Spadola, B. Bendinelli, E. Cocorocchio, I. Stanganelli, et al., Anti-hypertensive drugs and skin cancer risk: a review of the literature and meta-analysis, Crit. Rev. Oncol./Hematol. 122 (2018) 1–9.

[14] D.N. Syed, H. Mukhtar, Botanicals for the prevention and treatment of cutaneous melanoma, Pigment Cell Melanoma Res. 24 (4) (2011) 688–702.

[15] F.E. Alsaadi, M. Salman, M.U. Rehman, A.R. Khan, J. Cao, M.O. Alassafi, On the geodesic identification of vertices in convex plane graphs, Math. Probl. Eng. 2020 (2020) 1–13.

[16] A.R. Khan, A. Zia, F.J.H. Campeña, M.K. Siddiqui, F. Tchier, S. Hussain, Investigations of entropy double & strong double graph of silicon carbide, Silicon 16 (2024) 4187–4197.

[17] M.N. Husin, A.R. Khan, N.U.H. Awan, F.J.H. Campena, F. Tchier, S. Hussain, Multicriteria decision making attributes and estimation of physicochemical properties of kidney cancer drugs via topological descriptors, PLoS ONE 19 (5) (2024) e0302276.

[18] A.R. Khan, Z. Ullah, M. Imran, S.A. Malik, L.M. Alamoudi, M. Cancan, Molecular temperature descriptors as a novel approach for QSPR analysis of Borophene nanosheets, PLoS ONE 19 (6) (2024) e0302157.

[19] A.R. Khan, A. Mutlib, F.J.H. Campeña, F. Tchier, M. Karim, S. Hussain, Investigation of reduced reverse degree based polynomials & indices of gold crystals, Phys. Scr. 99 (2024) 075259.

[20] A.R. Khan, N.U.H. Awan, F. Tchier, S.D. Alahmari, A.F. Khalel, S. Hussain, An estimation of physiochemical properties of bladder cancer drugs via degree-based chemical bonding topological descriptors, J. Biomol. Struct. Dyn. (2023) 1–9.

[21] X. Zuo, M.F. Nadeem, M.K. Siddiqui, M. Azeem, Edge weight based entropy of different topologies of carbon nanotubes, IEEE Access 9 (2021) 102019–102029.

[22] M.U. Ghani, F. Sultan, E.S.M. Tag El Din, A.R. Khan, J.B. Liu, M. Cancan, A paradigmatic approach to find the valency-based K-Banhatti and redefined Zagreb entropy for niobium oxide and a metal–organic framework, Molecules 27 (20) (2022) 6975.

[23] A.R. Khan, M.U. Ghani, A. Ghaffar, H.M. Asif, M. Inc, Characterization of temperature indices of silicates, Silicon 15 (15) (2023) 6533–6539.

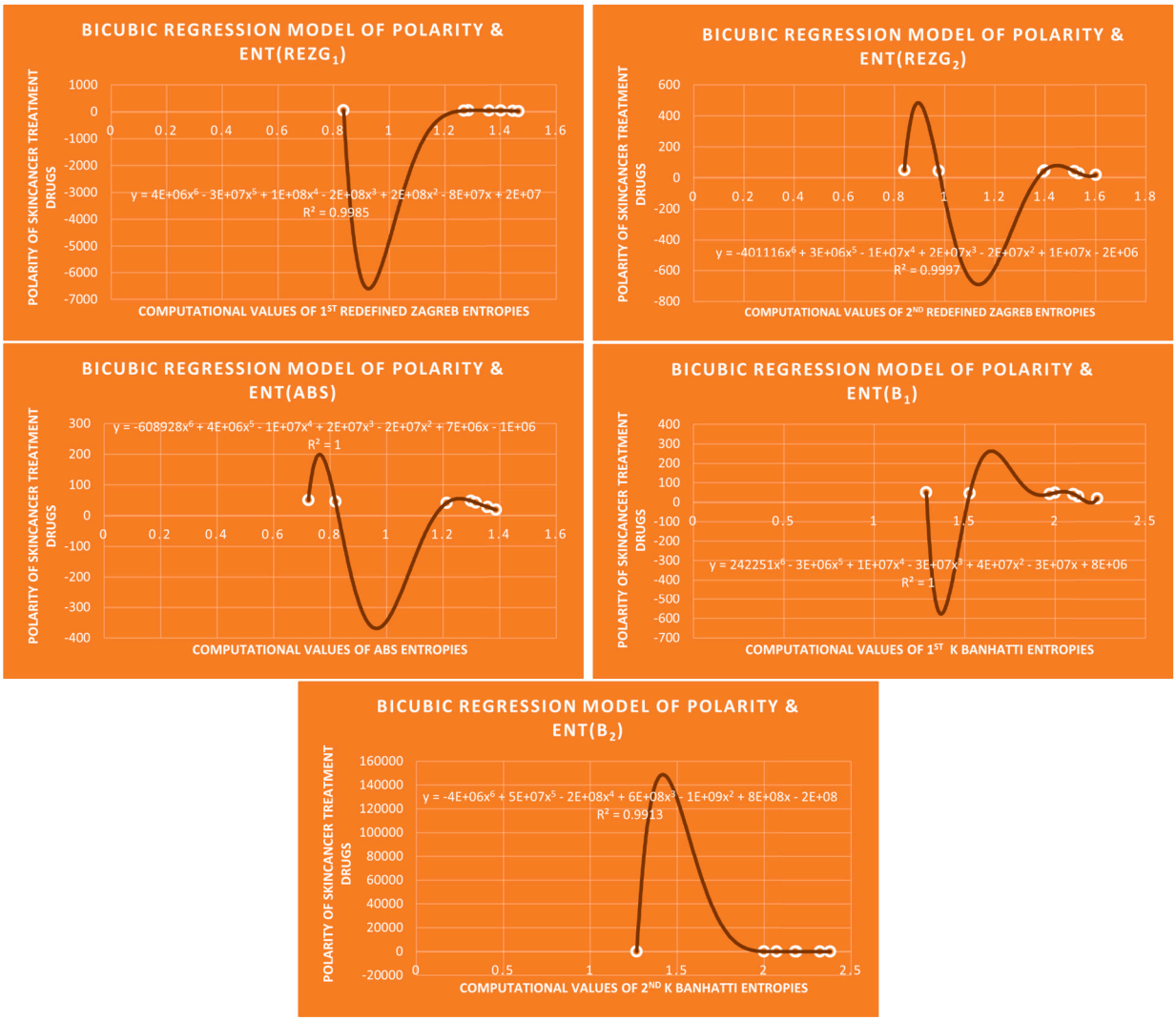

Fig. 8. BCR Models of Polarity.

[24] Z.H. Hui, M. Naeem, A. Rauf, A. Aslam, Predictive ability of physicochemical properties of antiemetic drugs using degree-based entropies, Int. J. Quant. Chem. e27131 (2023).
[25] P. Sarkar, N. De, A. Pal, On some topological indices and their importance in chemical sciences: a comparative study, Eur. Phys. J. Plus 137 (2) (2022) 195.
[26] A. Rauf, M. Naeem, J. Rahman, A.V. Saleem, QSPR study of Ve-degree based end Vertice edge entropy indices with physio-chemical properties of breast cancer drugs, Polycycl. Aromat. Compd. 43 (5) (2023) 4170–4183.
[27] D. Paul, M. Arockiaraj, K. Jacob, J. Clement, Multiplicative versus scalar multiplicative degree based descriptors in QSAR/QSPR studies and their comparative analysis in entropy measures, Eur. Phys. J. Plus 138 (4) (2023) 323.
[28] M. Arockiaraj, D. Paul, J. Clement, S. Tigga, K. Jacob, K. Balasubramanian, Novel molecular hybrid geometric-harmonic-Zagreb degree based descriptors and their efficacy in QSPR studies of polycyclic aromatic hydrocarbons, SAR QSAR Environ. Res. 34 (7) (2023) 569–589.
[29] M.P. Rahul, J. Clement, QSPR analysis of carbon allotropes by employing molecular descriptors and information entropies, Ain Shams Eng. J. 14 (11) (2023) 102542.
[30] J.S. Junias, J. Clement, M.P. Rahul, M. Arockiaraj, Two-dimensional phthalocyanine frameworks: topological descriptors, predictive models for physical properties and comparative analysis of entropies with different computational methods, Comput. Mater. Sci. 235 (2024) 112844.
[31] H. Wiener, Structural determination of paraffin boiling points, J. Am. Chem. Soc. 69 (1947) 17–20.
[32] D. Vukičević, M. Gašperov, Bond additive modeling 1. Adriatic indices, Croat. Chem. Acta 83 (2010) 243–260.
[33] V.R. Kulli, On K Banhatti indices of graphs, J. Comput. Math. Sci. 7 (2016) 213–218.
[34] V.R. Kulli, On K hyper-Banhatti indices and coindices of graphs, Int. Res. J. Pure Algebra 6 (2016) 300–304.
[35] V.R. Kulli, On multiplicative K Banhatti and multiplicative K hyper-Banhatti indices of V-Phenylenic nanotubes and nanotorus, Ann. Pure Appl. Math. 11 (2016) 145–150.
[36] P.S. Ranjini, V. Lokesha, A. Usha, Relation between phenylene and hexagonal squeeze using harmonic index, Int. J. Graph Theory 1 (2013) 116–121.
[37] A. Ullah, S. Zaman, A. Hamraz, Zagreb connection topological descriptors and structural property of the triangular chain structures, Phys. Scr. 98 (2) (2023) 025009.
[38] M. Imran, A.R. Khan, M.N. Husin, F. Tchier, M.U. Ghani, S. Hussain, Computation of entropy measures for metal-organic frameworks, Molecules 28 (12) (2023) 4726.

[39] Y.M. Chu, A.R. Khan, M.U. Ghani, A. Ghaffar, M. Inc, Computation of Zagreb polynomials and Zagreb indices for benzenoid triangular & hourglass system, Polycycl. Aromat. Compd. 43 (5) (2023) 4386–4395.
[40] A.R. Khan, S.A. Bhatti, M. Imran, F.M. Tawfiq, M. Cancan, S. Hussain, Computation of differential and integral operators using M-polynomials of gold crystal, Heliyon 10 (14) (2024) e34419.
[41] A.R. Khan, Z. Ullah, M. Imran, M. Salman, A. Zia, F. Tchier, S. Hussain, Degree-based topological indices and entropies of diamond crystals, Sci. Prog. 107 (3) (2024) 00368504241271719.
[42] K.J. Gowtham, M.N. Husin, Multiplicative reverse product connectivity and multiplicative reverse sum connectivity of silicate network, EDUCATUM J. Sci. Math. Technol. 10 (1) (2023) 90–100.
[43] C.E. Shannon, A mathematical theory of communication, Bell Syst. Tech. J. 27 (1948) 379–423.
[44] S.R.J. Kavitha, J. Abraham, M. Arockiaraj, J. Jency, K. Balasubramanian, Topological characterization and graph entropies of tessellations of kekulene structures: existence of isentropic structures and applications to thermochemistry, nuclear magnetic resonance, and electron spin resonance, J. Phys. Chem. A 125 (36) (2021) 8140–8158.
[45] S. Zaman, A. Ullah, Kemeny's constant and global mean first passage time of random walks on octagonal cell network, Math. Methods Appl. Sci. 46 (8) (2023) 9177–9186.
[46] A. Ullah, S. Zaman, A. Hamraz, G. Saeedi, Network-based modeling of the molecular topology of fuchsine acid dye with respect to some irregular molecular descriptors, J. Chem. 2022 (2022).
[47] S. Hayat, Computing distance-based topological descriptors of complex chemical networks: new theoretical techniques, Chem. Phys. Lett. 688 (2017) 51–58.
[48] S. Zaman, M. Jalani, A. Ullah, M. Ali, T. Shahzadi, On the topological descriptors and structural analysis of cerium oxide nanostructures, Chem. Pap. 77 (5) (2023) 2917–2922.
[49] J. Abraham, M. Arockiaraj, J. Jency, S.R.J. Kavitha, K. Balasubramanian, Graph entropies, enumeration of circuits, walks and topological properties of three classes of isoreticular metal organic frameworks, J. Math. Chem. 60 (4) (2022) 695–732.